

# Localizing in Urban Canyons using Joint Doppler and Ranging and the Law of Cosines Method

William W. Jun, *Georgia Institute of Technology*  
Kar-Ming Cheung, *Jet Propulsion Laboratory, California Institute of Technology*  
E. Glenn Lightsey, *Georgia Institute of Technology*  
Charles Lee, *Jet Propulsion Laboratory, California Institute of Technology*

## BIOGRAPHIES

William Jun graduated from the Georgia Institute of Technology in Atlanta, GA with a B.S. in Aerospace Engineering and a Minor in Computer Science, specializing in Artificial Intelligence. He started his work in navigation architectures during an internship at the NASA Jet Propulsion Laboratory (JPL) over the summer of 2018. Over the course of his time at Georgia Tech, he has worked in the Space Systems Design Laboratory (SSDL) contributing to various cube satellite missions as subsystem leads and as the Project Manager of Prox-1, which launched with STP-2 on a SpaceX Falcon Heavy's in 2019. He is continuing his education with a PhD at Georgia Tech under Dr. E. Glenn Lightsey, pursuing research in novel navigation architectures under the NASA Space Technology Research Fellowships (NSTRF).

Dr. Kar-Ming Cheung is a Principal Engineer and Technical Group Supervisor in the Communication Architectures and Research Section (332) at JPL. His group supports design and specification of future deep-space and near-Earth communication systems and architectures. Kar-Ming Cheung received NASA's Exceptional Service Medal for his work on Galileo's onboard image compression scheme. Since 1987, he has been with JPL where he is involved in research, development, production, operation, and management of advanced channel coding, source coding, synchronization, image restoration, and communication analysis schemes. He got his B.S.E.E. degree from the University of Michigan, Ann Arbor, in 1984, and his M.S. and Ph.D. degrees from California Institute of Technology in 1985 and 1987, respectively.

E. Glenn Lightsey is the David. S. Lewis Professor of Space Technology in the Daniel Guggenheim School of Aerospace Engineering at the Georgia Institute of Technology. He is the Director of the Center for Space Technology and Research and the Director of the Space Systems Design Lab at Georgia Tech. He previously worked at the University of Texas at Austin and NASA's Goddard Space Flight Center. His research program focuses on the technology of satellites, including: guidance, navigation, and control systems; attitude determination and control; formation flying and satellite swarms; cooperative control; proximity operations and unmanned spacecraft rendezvous; space based Global Positioning System receivers; radionavigation; visual navigation; propulsion; satellite operations; and space systems engineering. He has written 140 technical publications. He is an AIAA Fellow, and he serves as Associate Editor-in-Chief of the Journal of Small Satellites.

Professor Charles H. Lee received his Doctor of Philosophy degree in Applied Mathematics in 1996 from the University of California at Irvine. He then spent three years as a Post-Doctorate Fellow at the Center for Research in Scientific Computation, Raleigh, North Carolina, where he was the recipient of the 1997-1999 National Science Foundation Industrial Post-Doctorate Fellowship. He became an Assistant Professor of Applied Mathematics at the California State University Fullerton in 1999, Associate Professor in 2005, and since 2011 he has been a Full Professor. Dr. Lee has been collaborating with scientists and engineers at NASA Jet Propulsion Laboratory since 2000. His research has been Computational Applied Mathematics with emphases in Aerospace Engineering, Telecommunications, Acoustic, Biomedical Engineering and Bioinformatics. He has published over 65 professionally refereed articles. Dr. Lee received Outstanding Paper Awards from the International Congress on Biological and Medical Engineering in 2002 and the International Conference on Computer Graphics and Digital Image Processing in 2017. Dr. Lee also received NASA's Exceptional Public Achievement Medal in 2018 for the Development of his Innovative Tools to Assess the Communications & Architectures Performance of the Mars Relay Network.

## ABSTRACT

The performance of Global Navigation Satellite System (GNSS) based navigation can be limited in urban canyons and other regions with narrow satellite visibility. These regions may only allow for less than the minimum of four satellites to be visible, leading to a decay of positional knowledge. A scheme with Joint Doppler and Ranging (JDR) and relative positioning, known as the Law of Cosines (LOC) method, is introduced in this paper that utilizes Doppler and pseudorange measurements from a minimum of two GNSS satellites to obtain a position fix.

The user's GNSS receiver was assumed to output both corrected pseudorange and Doppler shift measurements for each tracked satellite. The velocity vector of each satellite was calculated using broadcast satellite ephemerides. Additionally, the location of the reference station was known and Doppler measurements from the GNSS receiver at the reference station were transmitted to the user.

Ephemerides from eight GNSS satellites were simulated with the user and reference station approximately 12 km apart in San Francisco. Gaussian error sources were modelled and randomized in Monte Carlo simulations, adding error to the receiver's known satellite ephemeris, satellite velocity, Doppler, and pseudorange measurements. Each unique pair of 2 satellites was employed for the positioning of the user using the LOC method for over 10,000 Monte Carlo simulations.

With reasonable assumptions on measurement error, the average 2D topocentric Root-Mean-Square-Error (RMSE) performance of all pairs of satellites was 23 meters, reducing to 10 meters by removing specific pairs with poor geometry. However, with a new technique called Terrain Assisted – JDR (TA-JDR), which uses accurate topographic information of the user's region as a faux pseudorange measurement, the average RSME of the satellite pairs was reduced to approximately 7 meters.

The use of the JDR-LOC scheme and its variants may not only be useful in urban canyons, but also in other GPS-denied unfriendly environments.

Ultimately, the JDR-LOC scheme was capable of achieving navigational solutions with an RMSE as low as 7 meters for users with limited GNSS satellite visibility, with only the use of a GNSS receiver and a reference station.

## INTRODUCTION

The Global Navigation Satellite System (GNSS), which includes the Global Positioning System (GPS), has been deemed successful through countless use-cases. These cases range from regular commercial and private use to research and military use [1]. However, at least four satellites in view are required for GNSS/GPS range measurements and some locations cannot utilize these positioning systems to their full potential. Urban canyons are locations where a user is surrounded by buildings which block GNSS signals and create a canyon-like environment. Positioning problems in these regions include a smaller quantity of visible satellites, multipath, and interference.

Temporary loss of GPS signals is caused by structures blocking line of sight to satellites, multipath and signal interference, thus lowering the number of usable satellites in urban environments. Various solutions have been proposed to resolve these issues, ranging from taking advantage of GLONASS systems [2], weighting models [3], shadow matching [4], and fuzzy logic [5]. However, the use of standard range-based trilateration is still assumed in these approaches. The Joint Doppler and Ranging Law of Cosines (JDR-LOC) scheme is reintroduced in this paper to enable relative positioning with as few as two satellites in view.

The Law of Cosines (LOC) scheme is a novel positioning scheme that only relies on Doppler measurements made by a user, a satellite(s), and a reference station [6]. Additional hardware or software is not required to obtain Doppler measurements; most GNSS receivers include options for logging Doppler shifts of locked satellites in real time. Therefore, positioning is enabled with relatively low hardware requirements and without the need for a clock bias calculation. However, improvements in performance have been shown with the addition of range measurements along with Doppler measurements. Range and Doppler measurements are integrated in the Joint Doppler and Ranging (JDR) scheme [7]. Additionally, the knowledge of the user's altitude was used as a pseudorange measurement from a faux satellite at the center of the planet. This faux measurement was known as the surface constraint [7].

Because ranging and Doppler measurements are based on independent states during an instantaneous timestep (position and velocity, respectively), two measurements can be provided by each satellite towards the calculation of position. Therefore, with the calculation of 3 Cartesian coordinates and a clock bias, only a minimum of two satellites are required for positioning. The JDR-LOC scheme is able to position a user in an urban canyon with only two satellites in view.

To test this theory, the user and reference station were assumed to be in San Francisco, separated by a distance of 12 km. All GPS satellites that were visible to the user at a certain epoch were found and their position and velocity vectors were exported from Systems Tool Kit. The position and velocity of the satellites were assumed to be known by the user (to a certain accuracy) through the orbital information broadcasted by each satellite.

The clock correction term for the user's clock was calculated in all analyses, enabling precise pseudorange measurements. The reference station's clock was synchronized with the GNSS/GPS. This could be assumed with a reference station on the top of a large hill or building, allowing it to see a large portion of the sky. Other errors, including ionospheric and tropospheric delays, were resolved using dual frequency measurements and the effects of relative navigation.

In simulation, the true pseudorange and Doppler measurements were calculated and then corrupted with Gaussian error. Additionally, the user's knowledge of each satellite's ephemeris and velocity vector were corrupted with Gaussian error. The reference station, which sends its Doppler measurements to the user, also had its measurements corrupted. Just as in other LOC analyses, the rough altitude of the user was assumed to be known and implemented as the surface constraint. All measurements and satellite knowledge were fed into the JDR-LOC scheme and used to calculate the user's position.

This entire process was repeated, with changes only to the Gaussian error with new, random values set by a given error standard deviation. This Monte Carlo simulation was repeated for 10,000 iterations. For each respective run of the JDR-LOC scheme, only two satellites were measured. This meant that all the unique pair combinations of the total 8 visible satellites were tested in each Monte Carlo iteration, totaling 28 pairs.

With the JDR-LOC scheme and reasonable assumptions on measurement error, the average 2D topocentric Root-Mean-Square-Error (RMSE) performance of all pairs of satellites was 23 meters, reducing to 10 meters by removing specific pairs with poor geometry.

Additionally, the use of a new technique called Terrain Assisted – JDR (TA-JDR) was introduced. A high resolution topographic map of the user's region was utilized in this new virtual instrument. After an initial position fix was calculated from the JDR-LOC scheme, the altitude of that calculated position was pulled from the topographic map and saved as a new surface constraint. The JDR-LOC scheme was run again with all the same measurements and parameters as last time, except with the new surface constraint. This process was repeated until the position fix converged to less than the resolution of the high-resolution topographic map. With TA-JDR, the vertical component of the position fix was resolved with additional information from a map. Additional measurements were not required and the accuracy of the user's height knowledge was increased. A caveat to this technique was that it did not account for a user not on the surface of the planet, such as in a high-rise building. With this new technique, the average RSME of the satellite pairs was reduced to approximately 7 meters.

Although this new approach to positioning with limited satellite resources was applied directly to GNSS in urban canyons, there are a myriad of applications of JDR-LOC and TA-JDR. For instance, JDR-LOC can be used to localize a rover on Mars or a user on the Lunar surface with two or even a single satellite (assuming two-way ranging). Additionally, with pre-existing high-resolution topographic maps of the Moon (e.g. the high-resolution Lunar Orbiter Laser Altimeter (LOLA) digital elevation map [8]), TA-JDR can be used to localize a user with greater accuracy than just the standard JDR-LOC. TA-JDR could also be used on other topics centered around JDR. Coupling an IMU is another area of research, which removes the requirement of a static user. Coupling an IMU with JDR through a Kalman filter is expected to improve performance of the scheme [9]. Positioning accuracy of these new schemes can be further improved with TA-JDR.

## JOINT DOPPLER AND RANGING LAW OF COSINES SCHEME (JDR-LOC)

The JDR-LOC scheme is a modification of the original LOC scheme including ranging measurements in addition to Doppler measurements [7]. A review of the JDR-LOC scheme was provided. The visualization of the user (T), the reference station (R), and one of the satellites (C) is described in Figure 1.

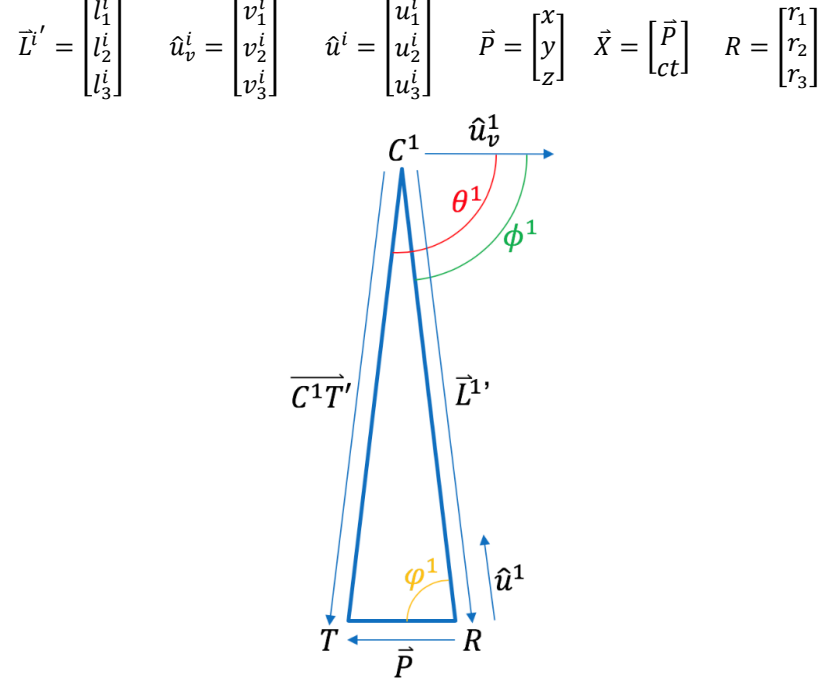


Figure 1: Visualization of the LOC Technique

$\hat{u}_v^i$  is the satellite's velocity vector, R is the reference station, T is the user, and C<sup>i</sup> is the current satellite

Using the Law of Cosines, a cost function was created (Eqn 1). This was the core cost function of the LOC scheme; the relative position P was calculated from the other input measurements.

$$f^i(x, y, z) = \left( \frac{\vec{L}^i \cdot \hat{u}_v^i}{\cos \phi^i} \right)^2 + \|\vec{P}\|^2 - 2 \left( \frac{\vec{L}^i \cdot \hat{u}_v^i}{\cos \phi^i} \right) (\vec{P} \cdot \hat{u}^i) - \left( \frac{(\vec{L}^i + \vec{P}) \cdot \hat{u}_v^i}{\cos \theta^i} \right)^2 \quad (\text{Eqn 1})$$

Additionally, the pseudorange measurement's equation was described as follows:

$$f^{i+n}(x, y, z) = \sqrt{\left( (x + r_1) - c_1^i \right)^2 + \left( (y + r_2) - c_2^i \right)^2 + \left( (z + r_3) - c_3^i \right)^2} + ct - PR^i \quad (\text{Eqn 2})$$

Where PR was the current satellite's pseudorange measurement. For the case of two satellites, or n = 2:

$$f(x, y, z) = \begin{bmatrix} \left( \frac{\vec{L}^1 \cdot \hat{u}_v^1}{\cos \phi^1} \right)^2 + \|\vec{P}\|^2 - 2 \left( \frac{\vec{L}^1 \cdot \hat{u}_v^1}{\cos \phi^1} \right) (\vec{P} \cdot \hat{u}^1) - \left( \frac{(\vec{L}^1 + \vec{P}) \cdot \hat{u}_v^1}{\cos \theta^1} \right)^2 \\ \left( \frac{\vec{L}^2 \cdot \hat{u}_v^2}{\cos \phi^2} \right)^2 + \|\vec{P}\|^2 - 2 \left( \frac{\vec{L}^2 \cdot \hat{u}_v^2}{\cos \phi^2} \right) (\vec{P} \cdot \hat{u}^2) - \left( \frac{(\vec{L}^2 + \vec{P}) \cdot \hat{u}_v^2}{\cos \theta^2} \right)^2 \\ \sqrt{\left( (x + r_1) - c_1^1 \right)^2 + \left( (y + r_2) - c_2^1 \right)^2 + \left( (z + r_3) - c_3^1 \right)^2} + ct - PR^1 \\ \sqrt{\left( (x + r_1) - c_1^2 \right)^2 + \left( (y + r_2) - c_2^2 \right)^2 + \left( (z + r_3) - c_3^2 \right)^2} + ct - PR^2 \end{bmatrix} \quad (\text{Eqn 3})$$

Then, the Jacobian of the cost function was calculated. The Jacobian elements for the cost functions (Equation 1) from the LOC scheme was described in Equation 4.

$$\begin{aligned}
\frac{\partial f_i}{\partial x} &= 2x - 2\|\vec{L}^i\|u_1^i - 2v_1^i \left( \frac{(l_1^i + x)v_1^i + (l_2^i + y)v_2^i + (l_3^i + z)v_3^i}{\cos^2 \theta^i} \right) \\
\frac{\partial f_i}{\partial y} &= 2y - 2\|\vec{L}^i\|u_2^i - 2v_2^i \left( \frac{(l_1^i + x)v_1^i + (l_2^i + y)v_2^i + (l_3^i + z)v_3^i}{\cos^2 \theta^i} \right) \\
\frac{\partial f_i}{\partial z} &= 2z - 2\|\vec{L}^i\|u_3^i - 2v_3^i \left( \frac{(l_1^i + x)v_1^i + (l_2^i + y)v_2^i + (l_3^i + z)v_3^i}{\cos^2 \theta^i} \right) \\
\frac{\partial f_i}{\partial ct} &= 0
\end{aligned} \tag{Eqn 4}$$

Along with the Jacobian elements for the pseudorange measurement equation, and with  $n = 2$  (Equation 5):

$$\begin{aligned}
&\text{Calculated Range} = \\
CR^i &= \sqrt{\left((x + r_1) - c_1^i\right)^2 + \left((y + r_2) - c_2^i\right)^2 + \left((z + r_3) - c_3^i\right)^2} \\
J(x, y, z) &= \begin{bmatrix} \frac{\partial f_1}{\partial x} & \frac{\partial f_1}{\partial y} & \frac{\partial f_1}{\partial z} & 0 \\ \frac{\partial f_2}{\partial x} & \frac{\partial f_2}{\partial y} & \frac{\partial f_2}{\partial z} & 0 \\ \frac{(x + r_1) - c_1^1}{CR^1} & \frac{(y + r_2) - c_2^1}{CR^1} & \frac{(z + r_3) - c_3^1}{CR^1} & 1 \\ \frac{(x + r_1) - c_1^2}{CR^2} & \frac{(y + r_2) - c_2^2}{CR^2} & \frac{(z + r_3) - c_3^2}{CR^2} & 1 \end{bmatrix}
\end{aligned} \tag{Eqn 5}$$

Finally, the surface constraint equation is as follows:

$$\begin{aligned}
&SC = \text{surface constraint} \\
f^{i+2n}(x, y, z) &= (x + r_1)^2 + (y + r_2)^2 + (z + r_3)^2 - SC * SC
\end{aligned} \tag{Eqn 6}$$

And the respective updated cost functions and Jacobians with only two satellites ( $n = 2$ ):

$$f(x, y, z) = \begin{bmatrix} \left( \frac{\vec{L}^1 \cdot \hat{u}_v^1}{\cos \phi^1} \right)^2 + \|\vec{P}\|^2 - 2 \left( \frac{\vec{L}^1 \cdot \hat{u}_v^1}{\cos \phi^1} \right) (\vec{P} \cdot \hat{u}^1) - \left( \frac{(\vec{L}^1 + \vec{P}) \cdot \hat{u}_v^1}{\cos \theta^1} \right)^2 \\ \left( \frac{\vec{L}^2 \cdot \hat{u}_v^2}{\cos \phi^2} \right)^2 + \|\vec{P}\|^2 - 2 \left( \frac{\vec{L}^2 \cdot \hat{u}_v^2}{\cos \phi^2} \right) (\vec{P} \cdot \hat{u}^2) - \left( \frac{(\vec{L}^2 + \vec{P}) \cdot \hat{u}_v^2}{\cos \theta^2} \right)^2 \\ \sqrt{\left((x + r_1) - c_1^1\right)^2 + \left((y + r_2) - c_2^1\right)^2 + \left((z + r_3) - c_3^1\right)^2} + ct - PR^1 \\ \sqrt{\left((x + r_1) - c_1^2\right)^2 + \left((y + r_2) - c_2^2\right)^2 + \left((z + r_3) - c_3^2\right)^2} + ct - PR^2 \\ (x + r_1)^2 + (y + r_2)^2 + (z + r_3)^2 - SC^2 \end{bmatrix} \tag{Eqn 7}$$

$$J(x, y, z) = \begin{bmatrix} \frac{\partial f_1}{\partial x} & \frac{\partial f_1}{\partial y} & \frac{\partial f_1}{\partial z} & 0 \\ \frac{\partial f_2}{\partial x} & \frac{\partial f_2}{\partial y} & \frac{\partial f_2}{\partial z} & 0 \\ \frac{(x + r_1) - c_1^1}{CR^1} & \frac{(y + r_2) - c_2^1}{CR^1} & \frac{(z + r_3) - c_3^1}{CR^1} & 1 \\ \frac{(x + r_1) - c_1^2}{CR^2} & \frac{(y + r_2) - c_2^2}{CR^2} & \frac{(z + r_3) - c_3^2}{CR^2} & 1 \\ \frac{2(x + r_1)}{2(x + r_1)} & \frac{2(y + r_2)}{2(y + r_2)} & \frac{2(z + r_3)}{2(z + r_3)} & 0 \end{bmatrix} \quad (\text{Eqn 8})$$

The forms of Equation 7 and 8 that were implemented into the simulation were modified to move all of the cosine terms into a numerator to reduce the divergent effects of dividing by zero. These forms (Eqn 7 – 8) were shown for clarity.

## SCENARIO

### User and Reference Station

As a quintessential example of the effects of urban canyons, San Francisco was used for the user's location. Having the reference station 12 km away from the user (Table 1), a communications link established with the user, and the ability to see the same satellites that would be visible to the user are requirements for the LOC scheme. These requirements could be accomplished with a reference station on the top of a large hill or building, allowing it to see a large portion of the sky while also being close enough to the user for communications. It was assumed that the user was static or moving at a slow speed because of the reliance on Doppler measurements, which are dependent on the user's velocity. The use of a coupled IMU, correcting for a non-zero user velocity, will be described in future work [9].

Table 1: User and Reference Station Locations

Name	Location
User	37.767992° N, -122.444140° W
Reference Station	37.780543° N, -122.308534° W

### GPS Satellites

All current GPS satellites were modelled into Systems Tool Kit (STK) at the epoch of Nov 6<sup>th</sup>, 2018 17:00 to calculate access with a user on the ground. All satellites without access to the user were suppressed (Figure 2).

The state of each visible satellite (ephemeris and velocity in ECEF) were exported at the epoch, along with the Cartesian ECEF location of the user. These were used to calculate the Doppler count that the user would expect from each satellite at that time point. Approximately 8 satellites were visible (above an elevation mask) by the user at this time, so every combination of two visible satellites were tested in this analysis.

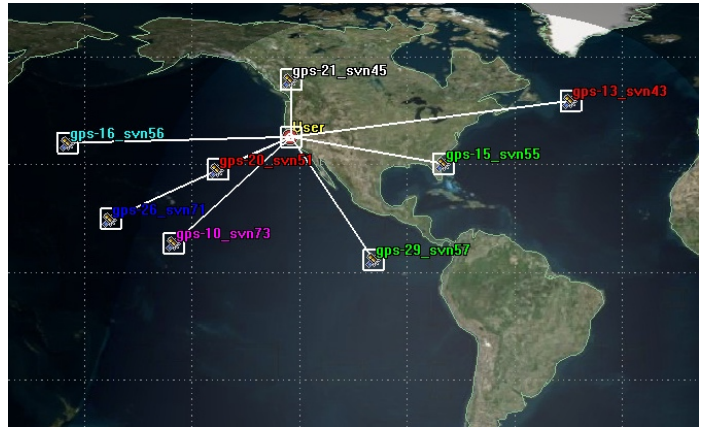
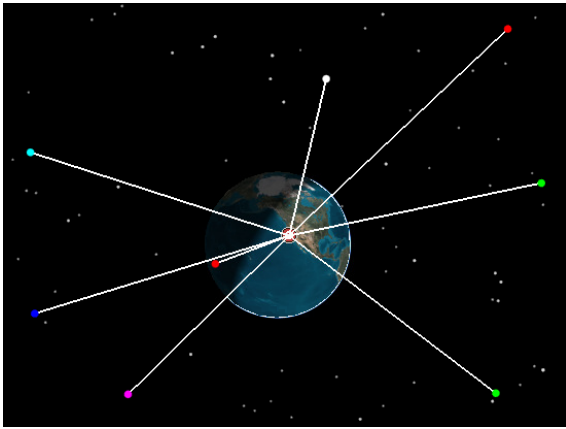


Figure 2: Visualization of All Satellites with Line of Sight Access to User [10]

### Measurement Calculation and Additional Gaussian Error

With the known satellite ephemeris and velocity, ideal pseudorange measurements and Doppler count measurements were calculated and then corrupted with Gaussian error (Table 2), also corrupting the user's ephemeris and velocity knowledge. The Doppler measurements were calculated using the standard L1 transmitting frequency for GPS: 1575.42 MHz.

Table 2:  $1\sigma$  Gaussian Error Values

Error Type	$1\sigma$ Value
Satellite Ephemeris Vector (3D)	5 m
Satellite Velocity Vector (3D)	1 mm/s
Pseudorange Measurement	5 cm
Doppler Count	0.00075 Hz

### SIMULATION AND RESULTS

To simulate the blockage of satellite line of sights in an urban canyon, only a single pair of satellites was used in each execution of the JDR-LOC scheme. All combinations of unique satellite pairs were calculated, totaling to 28 unique pairs:

Table 3: All Unique Pairs of the 8 Visible GPS Satellites

10-13	10-21	13-16	13-29	15-26	16-26	20-29
10-15	10-26	13-20	15-16	15-29	16-29	21-26
10-16	10-29	13-21	15-20	16-20	20-21	21-29
10-20	13-15	13-26	15-21	16-21	20-26	26-29

With each unique pair, all of the ephemeris and velocity data was simulated at the epoch and their respective Doppler and pseudorange measurements were calculated. These were used as the input to a Monte Carlo simulation, with the Gaussian error on all parameters listed in Table 2 recalculated over 10,000 iterations.

The results of each iteration were summarized onto Figure 3. The average error over all 10,000 iterations was stated as the "Mean Error", with the  $1\sigma$  standard deviation described with error bars. The root mean squared (RMS) error, which accumulated both the mean and standard deviation, was also shown as an addition to the mean error.

Figure 4 took the same results of each iteration and converted them into a 2D form; latitude and longitude. Because this removed the height component of the user's position, it also removed any errors associated with the calculated height. Therefore, the errors slightly decreased.

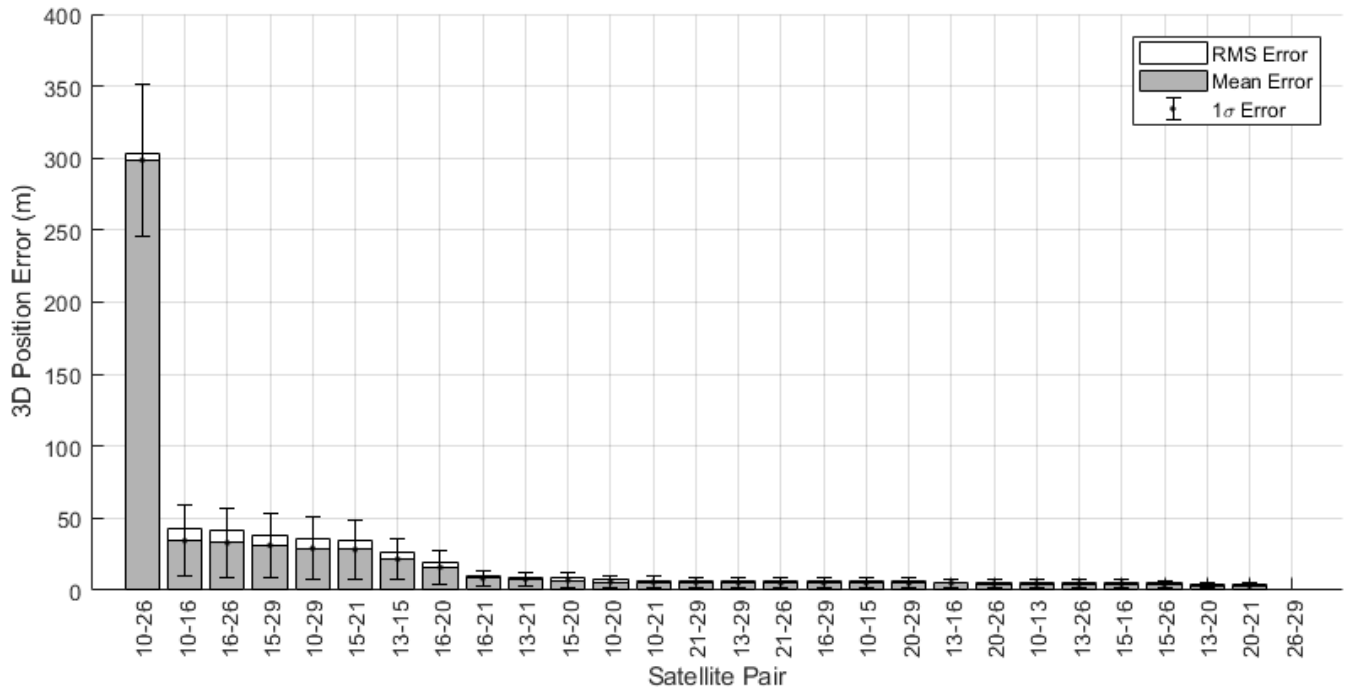


Figure 3: JDR-LOC 3D Positioning Errors for Each Satellite Pair (Sorted by RMSE)  
**Average RMSE: 24.4829 m**

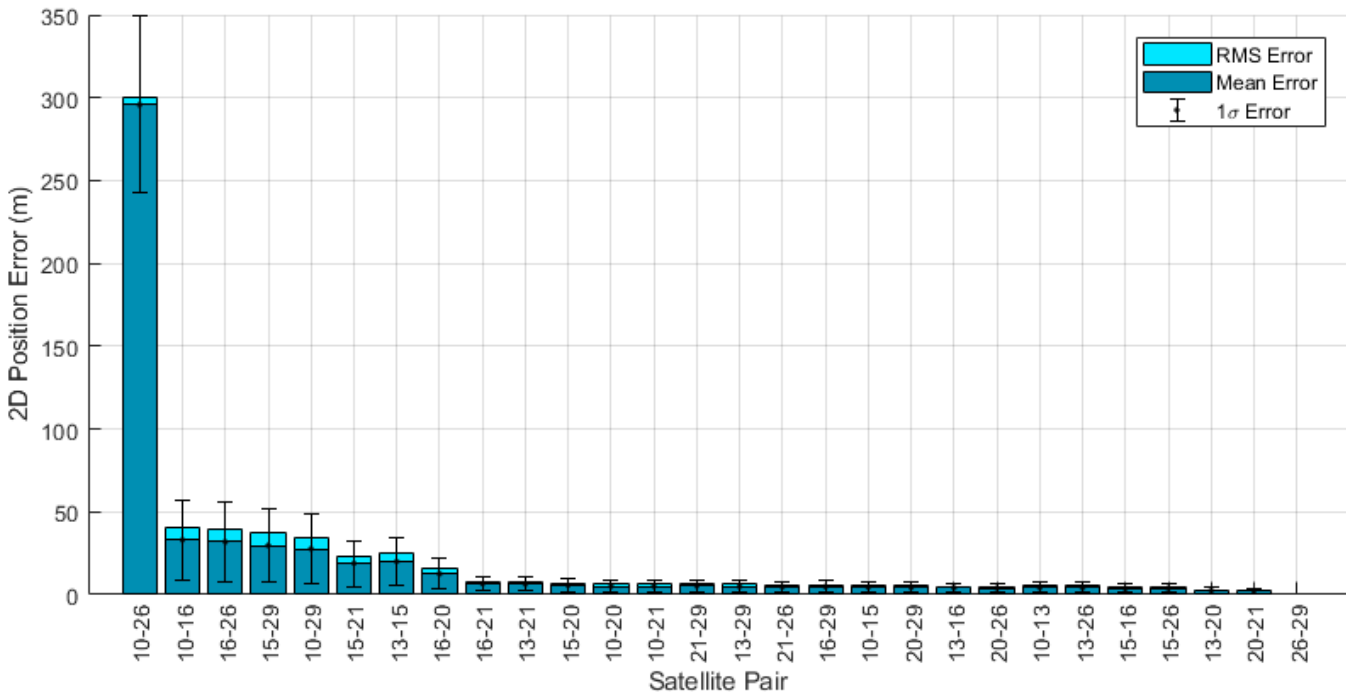


Figure 4: JDR-LOC 2D Positioning Errors for Each Satellite Pair (Pair order set by Figure 3)  
**Average RMSE: 23.0463 m**

As can be seen in Figures 3 and 4, some specific satellite pairs result in consistently higher errors than others. This can be explained through dilution of precision (DOP), the angle between each satellite in the sky from the user's perspective, and the angle between the satellites' velocity vectors.



From the perspective of the user on the surface of the planet, the distance between each satellite pair in the sky – converted to an angle - was calculated. This angle was used in addition to the DOP to easily understand of the geometry of the system. Because the JDR scheme relies on the Doppler measurement, the angle between the velocity vectors of each satellite in the pair were also calculated.

For each satellite pair, the minimum between the position vector angles and the velocity vector angles was chosen and displayed in the top plot of Figure 5. Additionally, the JDR-LOC scheme was run with no additional error, resulting in the error baseline for the system (bottom plot of Figure 5).

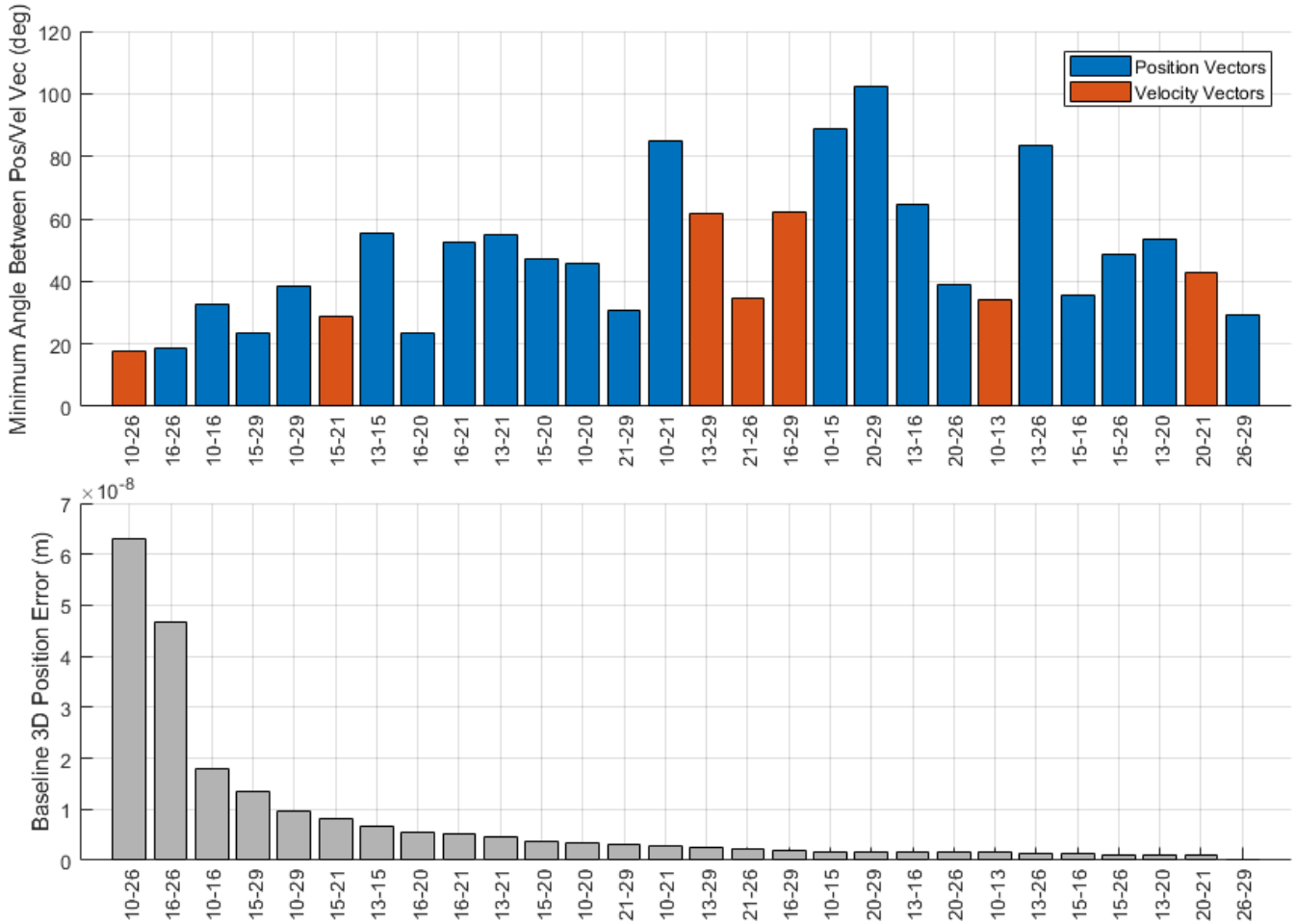


Figure 5: Minimum Angle (Position or Velocity) for Each Satellite Pair (TOP) and the Baseline 3D Position Error for JDR-LOC for Each Satellite Pair (BOTTOM)

As shown in Figure 5, the spikes in error for the JDR-LOC error baseline aligned with the dips in minimum angles. This can be explained with both the angles between satellite positions and the angles between satellite velocity vectors. If the satellite pair chosen were close to each other in the sky (therefore with a smaller angle between them), the range measurements would be fairly similar, decreasing data diversity. This was essentially the same as having a large DOP with 4 or more satellites. Additionally, if the angles between the velocity vectors were small, the Doppler measurements observed by both the satellites were similar, further decreasing data diversity. Because of this, all pairs of satellites with angles less than 25 degrees for either satellite position or velocity vectors was deemed a “high DOP pair” and removed from analysis. Additionally, pairs with DOPs that were outliers were removed. Because these decisions were based off of only the satellite ephemeris and velocity vectors, these “high DOP pairs” can be predicted and removed completely and/or weighted lower in a filter.

The same results that are shown in Figures 3 and 4 are displayed in Figures 6 and 7 with the high DOP pairs removed.

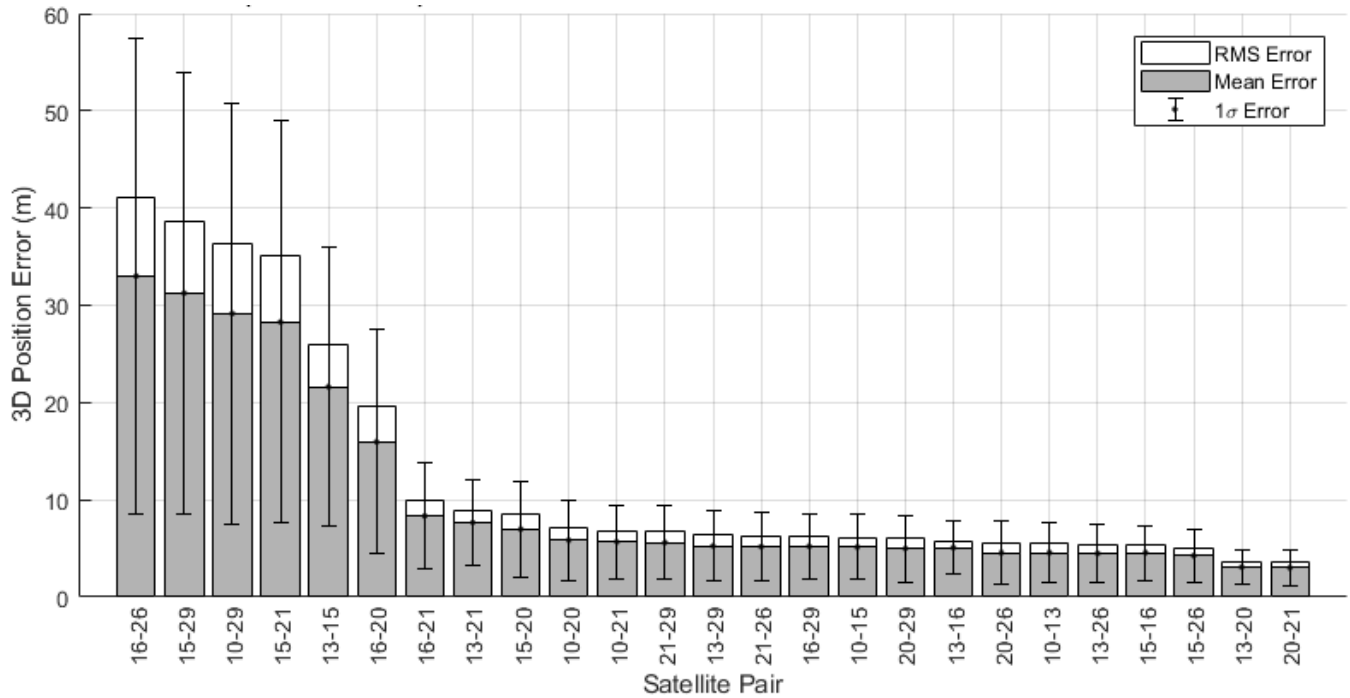


Figure 6: JDR-LOC 3D Positioning Errors for Each Satellite Pair (Sorted by RMSE) with High DOP Pairs Removed  
Average RMSE: 12.6159 m

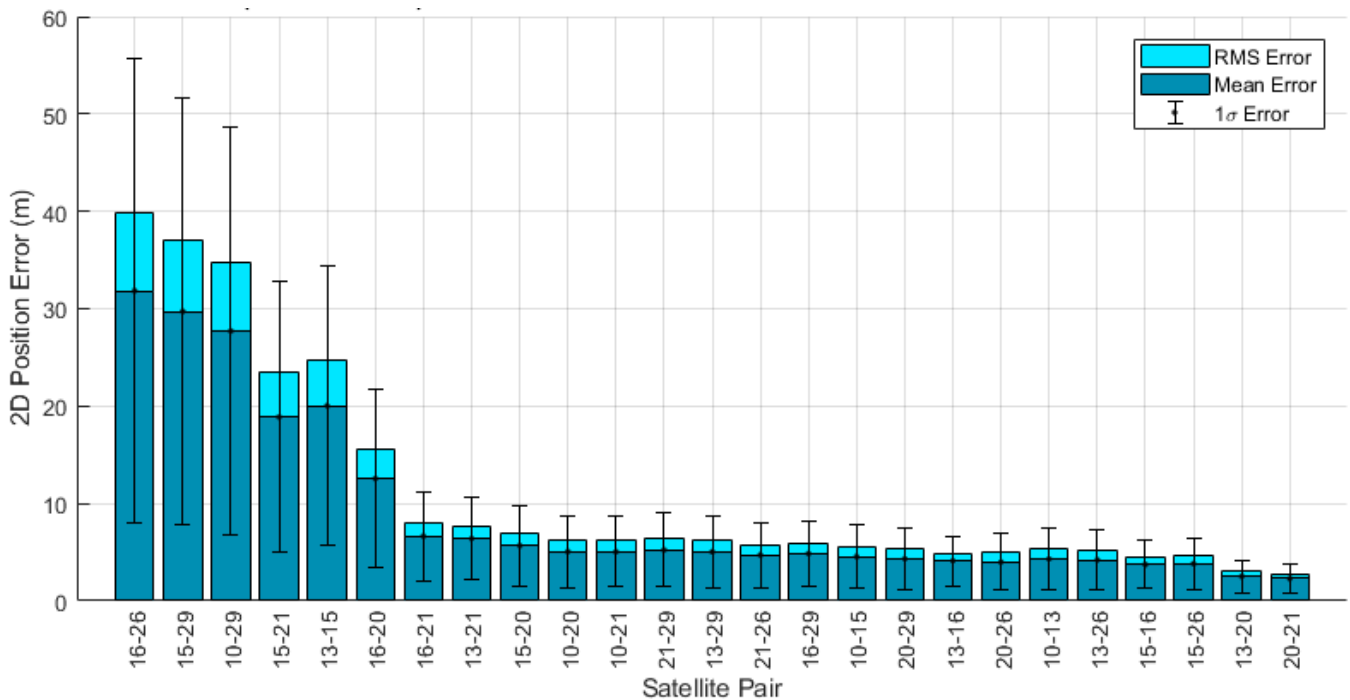


Figure 7: JDR-LOC 2D Positioning Errors for Each Satellite Pair (Pair order set by Figure 6) with High DOP Pairs Removed  
Average RMSE: 11.2343 m

Ultimately, with removing high DOP pairs and over 10,000 Monte Carlo iterations, the average RMSE over the remaining pairs were found to be 12.6159 meters, reducing to 11.2343 meters when converting to a 2D position.

## TERRAIN ASSISTED - JOINT DOPPLER AND RANGING (TA-JDR)

As stated in the Introduction, the use of a new technique called Terrain Assisted – JDR (TA-JDR) is introduced in this paper. A high resolution topographic map of the user’s region is utilized in this technique by iterating between parsing the topographic map and calling the JDR-LOC scheme to converge on a final position. One thing to note was that no new measurements were required for TA JDR; the measurements taken for the original execution of the JDR-LOC scheme were reused in TA-JDR to converge on a new position. This meant that only computational complexity (not hardware) was increased. Additionally, TA-JDR can be implemented anytime a JDR scheme is used (as long as a topographic map of the region exists). However, a caveat to this technique was that it assumed the user was on the surface of the planet; this assumption does not hold if the user is not on the surface of the topographic map, such as in a high-rise building.

First, a topographic map of the region was simulated. A true map of San Francisco could have been used in place of this simulated map, but simulation allowed for flexibility in terms of the map’s resolution, gradient, and size. The general change in altitude of a 1 km<sup>2</sup> region in downtown San Francisco was found to vary from approximately 10 m to 100 m [11]. Therefore a 1 km<sup>2</sup> region varying in height by approximately 100 m was simulated, with a resolution of 1 meter (Figure 8). The center of the map was assumed to be the true user position.

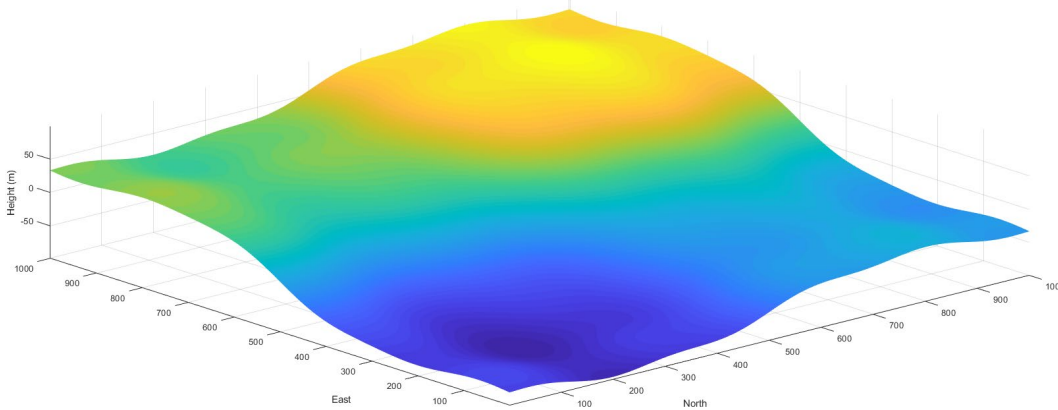


Figure 8: Simulated Topographic Map of User’s Region

First, the JDR-LOC scheme was run with measurements taken at a time epoch. The satellite ephemeris, velocity, Doppler measurements, and pseudorange measurements at the same epoch, in addition to the JDR-LOC position fix calculated in the JDR-LOC scheme were used as the starting points for the new TA-JDR-LOC analysis. With the calculated position fix, the topographic map was parsed, and the altitude of that position fix was saved as a new surface constraint. Then, the JDR-LOC scheme was executed again with the same measurements and parameters at the original epoch, except with the new surface constraint and initial position. This process was repeated until the position fix was found to converge to less a meter (the resolution of the map). This system was described in Figure 9.  $r^{FIX}$  is the position fix in the Fixed frame (FIX), and  $r^{NED}$  is in the North East Down frame (NED).  $C_{NED}^{FIX}$  is a transformation from NED to FIX, with  $C_{FIX}^{NED}$  from FIX to NED.

With TA-JDR, the average 3D RMSE of all satellite pairs was less than the average 2D RMSE of all the satellite pairs only using the JDR-LOC scheme (Figure 10: 19.1444 m vs. 23.0463 m). Utilizing the knowledge of high DOP pairs to remove the outliers, the total RMSE was reduced to 7.3761 meters, with a majority of satellite pairs resulting in errors under 5 meters (Figure 11).

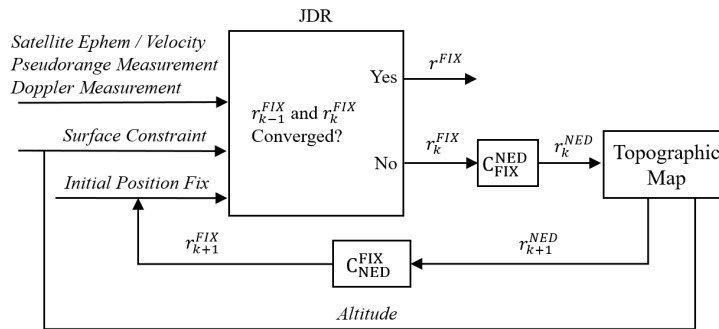


Figure 9: TA JDR Block Diagram

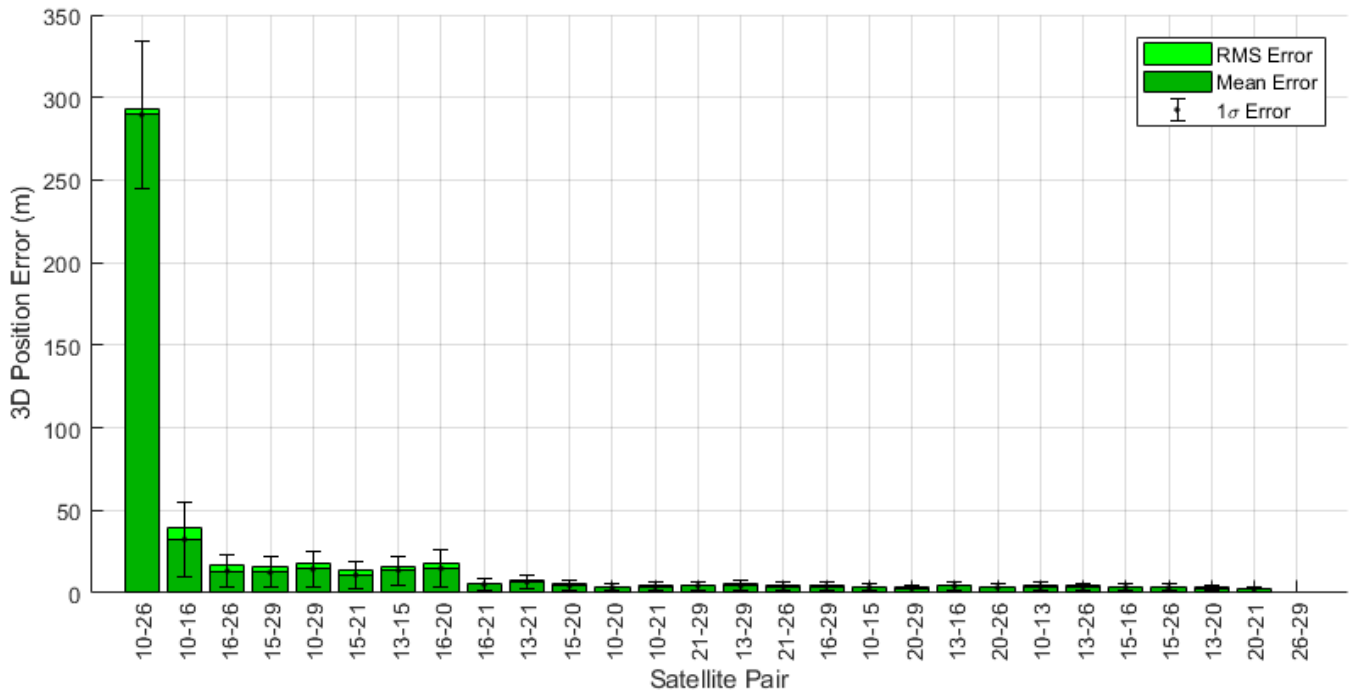


Figure 10: TA JDR-LOC 3D Positioning Errors for Each Satellite Pair (Pair order set by Figure 3)  
**Average RMSE: 19.1444 m**

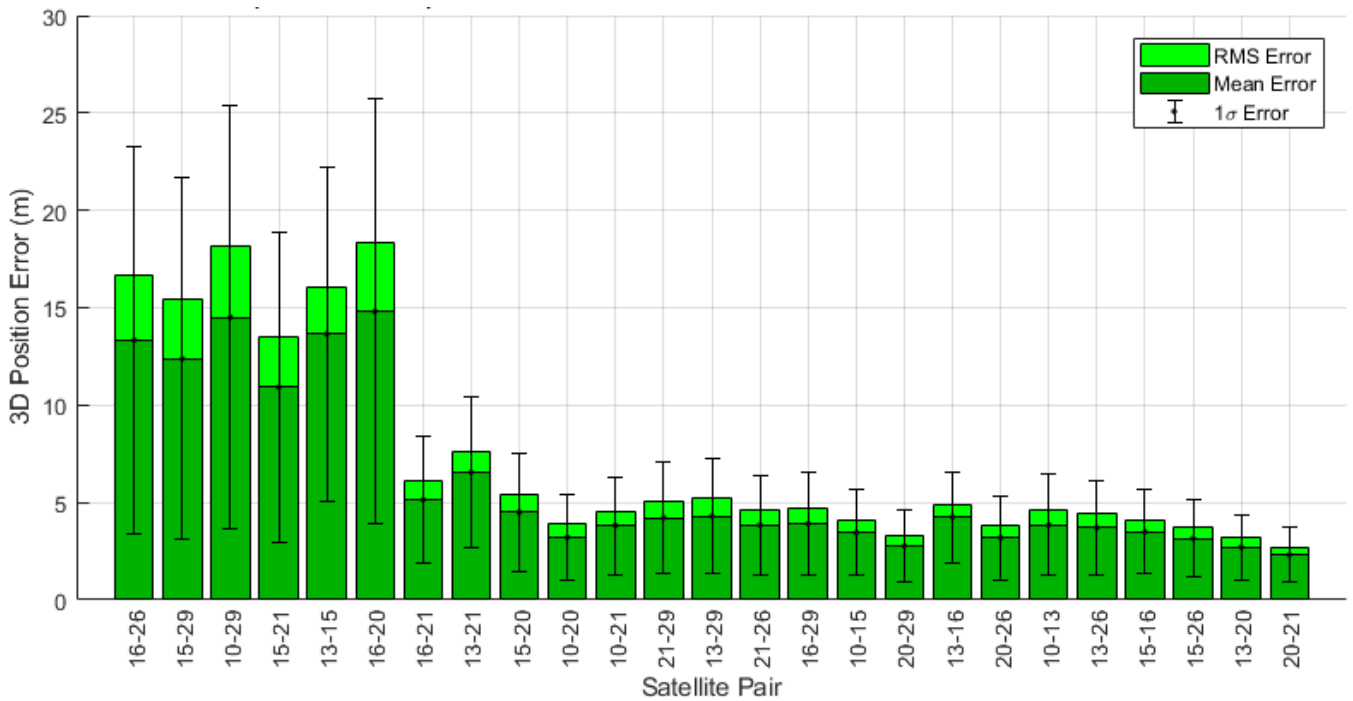


Figure 11: TA JDR-LOC 3D Positioning Errors for Each Satellite Pair (Pair order set by Figure 6)  
 with High DOP Pairs Removed  
**Average RMSE: 7.3761 m**

## CONCLUSIONS

This paper described the use of the JDR-LOC scheme to obtain position fixes during times with a minimum of two satellites in view. Situations with only a few visible satellites may be prevalent in urban canyons, where structures can block line of sight, cause multipath, and where signal interference may be an issue.

With only observing two satellites at a time and using reasonable assumptions on measurement error, a Monte Carlo simulation was performed to observe the performance of the JDR-LOC scheme with GPS. The average 2D topocentric Root-Mean-Square-Error (RMSE) performance of all pairs of satellites was approximately 24 meters, reducing to 12 meters by removing specific pairs with poor geometry. Therefore, with only two satellites in view and a reference station, a user could be localized within 12 meters from their true position.

Additionally, this paper introduced the use of a new technique called Terrain Assisted – JDR (TA-JDR). This new virtual instrument utilized a high resolution topographic map and the same measurements taken for JDR-LOC to converge on an improved position. The TA-JDR technique can be used with any JDR scheme as long as an accurate topographic map is present. With TA-JDR, the average 3D RMSE was approximately 19 meters, reducing to 7 meters by removing high DOP satellite pairs.

Situations other than urban canyons can warrant the use of JDR-LOC and TA-JDR, such as in GPS denied environments or even during navigation on other planets where the number of satellites is limited. For instance, JDR-LOC could be used to localize a rover on Mars with two satellites in view and a reference station (such as a static lander). Additionally, JDR-LOC could be used to localize a user on the Lunar surface with a reference station and two or even only a single satellite (assuming two-way ranging). With the pre-existing high fidelity topographic maps of the Moon, TA-JDR could be used to increase accuracy even further.

Finally, TA-JDR would improve the ongoing work with IMU coupled JDR schemes [9]. Future work includes observing the effects of increasing the number of visible satellites to 3, observing the performance of both schemes with time variant scenarios, performing hardware in the loop tests, and analyzing scenarios on other planets such as the Moon and Mars.

Ultimately, these novel approaches to positioning can enable and improve navigation on Earth and beyond.

## ACKNOWLEDGMENTS

The research described in this paper was carried out at the Jet Propulsion Laboratory, California Institute of Technology, under a contract with the National Aeronautics and Space Administration. The research was supported by NASA's Space Communication and Navigation (SCaN) Program.

## REFERENCES

1. K. Novak and J. D. Bossler, "Development and Application of the Highway Mapping System of Ohio State University," *The Photogrammetric Record*, Vol. 15. No. 85, 1995.
2. M. Tsakiri, A. Kealy, and M. Stewart, "Urban Canyon Vehicle Navigation with Integrated GPS / GLONASS / DR Systems," *NAVIGATION*, Vol. 46, No. 3, 1999, pp. 161-174.
3. S. Tay and J. Marais, "Weighting models for GPS Pseudorange observations for land transportation in urban canyons," *6th European Workshop on GNSS Signals and Signal Processing*, 2013, pp. 4.
4. S. Syed and M. E. Cannon, "Fuzzy Logic Based-Map Matching Algorithm for Vehicle Navigation System in Urban Canyons," *ION National Technical Meeting, San Diego, CA*, 2004
5. P. D. Groves, "Shadow Matching: A New GNSS Positioning Technique for Urban Canyons," *The Journal of Navigation*, Vol 64. 2011, pp. 417-430.
6. K. Cheung, W. W. Jun, C. Lee, E. G. Lightsey, "Single-Satellite Doppler Localization with Law of Cosines (LOC)," *2019 IEEE Aerospace Conference, Big Sky, MT*, 2019.
7. K. Cheung, W. W. Jun, E. G. Lightsey, C. Lee, T. Stevenson, "Single-Satellite Real-Time Relative Localization Using Joint Doppler and Ranging (JDR)", *70th International Astronautical Congress 2019*, October 2019.

8. M. K. Barker, E. Mazarico, G. A. Neumann, M. T. Zuber, J. Haruyama, D. E. Smith, "A new lunar digital elevation model from the Lunar Orbiter Laser Altimeter and SELENE Terrain Camera," *Icarus*, Volume 273, pp. 346-355.
9. W. W. Jun, K. Cheung, J. Milton, E. G. Lightsey, C. Lee, "Autonomous Navigation for Crewed Lunar Missions with DBAN", *2020 IEEE Aerospace Conference*, Big Sky, MT, *To be presented*.
10. Analytical Graphics Inc., "Systems Tool Kit" [Computer Software], *Analytical Graphics Inc.*
11. DataSF. "Elevation Contours," *Energy and Environment*. <https://data.sfgov.org/Energy-and-Environment/Elevation-Contours/rnbg-2qxw>